Developmental Biology 317 (2008) 695–704

Contents lists available at ScienceDirect

Developmental Biology

journal homepage: www.elsevier.com/developmentalbiology

Genomes & Developmental Control

Identification of *cis*-regulatory elements from the *C. elegans* T-box gene *mab-9* reveals a novel role for *mab-9* in hypodermal function

Peter J. Appleford, Maria Gravato-Nobre, Toby Braun, Alison Woollard *

Genetics Unit, Department of Biochemistry, University of Oxford, South Parks Road, Oxford OX1 3QU, UK

ARTICLE INFO

Article history:
Received for publication 8 October 2007
Revised 14 February 2008
Accepted 23 February 2008
Available online 18 March 2008

Keywords:
C. elegans
T-box
mab-9
Hypodermis
cis-regulation

ABSTRACT

We have identified Conserved Non-coding Elements (CNEs) in the regulatory region of *Caenorhabditis elegans* and *Caenorhabditis briggsae mab-9*, a T-box gene known to be important for cell fate specification in the developing *C. elegans* hindgut. Two adjacent CNEs (a region 78 bp in length) are both necessary and sufficient to drive reporter gene expression in posterior hypodermal cells. The failure of a genomic *mab-9*::*gfp* construct lacking this region to express in posterior hypodermis correlates with the inability of this construct to completely rescue the *mab-9* mutant phenotype. Transgenic males carrying this construct in a *mab-9* mutant background exhibit tail abnormalities including morphogenetic defects, altered tail autofluorescence and abnormal lectin-binding properties. Hermaphrodites display reduced susceptibility to the *C. elegans* pathogen *Microbacterium nematophilum*. This comparative genomics approach has therefore revealed a previously unknown role for *mab-9* in hypodermal function and we suggest that MAB-9 is required for the secretion and/or modification of posterior cuticle.

Introduction

The *mab-9* mutation was originally identified in a screen for worms defective in mating (Hodgkin, 1983). In the developing hindgut of wild-type (WT) *Caenorhabditis elegans*, MAB-9 acts to specify the identity of the male-specific blast cells B and F; in *mab-9* mutants, B and F assume the fates of their two anterior neighbours, Y and U, resulting in grossly abnormal male tails lacking many of the normal internal structures (Chisholm and Hodgkin, 1989). In hermaphrodites this hindgut defect leads to severe constipation because B and F are required for the structural integrity of the rectum. In addition to hindgut and tail abnormalities, *mab-9* worms are defective for backward movement (Chisholm and Hodgkin, 1989; Woollard and Hodgkin, 2000). This is now known to be caused by an axon guidance defect in which *mab-9* mutants fail to correctly form circumferential commissures from the ventral nerve cord (VNC) (Huang et al., 2002; Pocock et al., unpublished). *mab-9* encodes a member of the Tbx20 sub-family of T-box transcriptional regulators (Woollard and Hodgkin, 2000). T-box genes are widely distributed in nature with various developmental roles (reviewed in Papaioannou, 2001) and mutations in a number of T-box genes have been linked to human developmental disorders, including DiGeorge syndrome, Holt–Oram syndrome and Ulnar–Mammary syndrome (reviewed in Packham and Brook, 2003).

We have previously shown that a *mab-9*::*gfp* construct including approximately 5.5 kb of upstream sequence was able to completely rescue the *mab-9* phenotype, indicating that this region includes all regulatory sequences required for correct MAB-9 expression (Woollard and Hodgkin, 2000). Worms rescued with this transgene exhibit GFP expression in nuclei of the rectal epithelial cells B and F (and B- and F-derived cells in males), a subset of ventral nerve cord nuclei and a single head neuron (Woollard and Hodgkin, 2000; Pocock et al., unpublished), as well as 3 or 4 nuclei of the posterior hypodermis.

Since MAB-9 is expressed in a variety of different tissues and performs a number of disparate functions in *C. elegans*, we were interested in dissecting the regulatory region in order to define precise regulatory elements. Study of gene regulation in *C. elegans* is now greatly facilitated by the availability of the genome sequence of the closely related species *Caenorhabditis briggsae*. Although the degree of conservation between the two genomes is generally high for coding sequences, there is generally less conservation outside of coding regions (Stein et al., 2003). Blocks of Conserved Non-coding Elements (CNEs) are thought to be likely domains of gene regulation, by acting as binding sites for trans-acting factors (Wang et al., 1999; Kirouac and Sternberg, 2003).

Here we show that there are six CNEs shared between *C. elegans mab-9* and its nearest *C. briggsae* homologue, *CBG24273*. Firstly, we demonstrate that *CBG24273* is a probable *mab-9* orthologue by comparing expression patterns and rescuing ability. Secondly, deletion of CNEs from the *C. elegans mab-9* rescuing construct reveals two adjacent blocks of homologous sequence comprising a total of 78 bp that are absolutely required for expression in the posterior hypodermis. These sequences are also sufficient to drive hypodermal expression of a GFP reporter when inserted into an expression vector containing minimal promoter elements from the embryonically-

* Corresponding author. Fax: +44 1865 275318.
E-mail addresses: alison.woollard@bioch.ox.ac.uk, rachael.nimmo@linacre.ox.ac.uk (A. Woollard).

0012-1606/$ – see front matter © 2008 Elsevier Inc. All rights reserved.
doi:10.1016/j.ydbio.2008.02.049

expressed gene *pes-10* (Seydoux and Fire, 1994). *mab-9* mutant animals containing a construct lacking this 78 bp region are not completely rescued and exhibit several male-specific defects including abnormal cuticle properties. *mab-9* hermaphrodites containing the same construct exhibit reduced susceptibility to infection by the pathogenic bacterium *Microbacterium nematophilum* because bacteria are less able to colonise the rectum of worms lacking posterior hypodermal expression of MAB-9. Thus, our studies reveal a novel role for *mab-9* in hypodermal function in both males and hermaphrodites. This aspect of *mab-9* function would not be revealed in loss-of-function mutants due to the severe morphological defects in such alleles masking more subtle defects in hypodermal morphogenesis and cuticle function.

Materials and methods

Strains and worm maintenance

All *C. elegans* strains used were derived from the wild-type (WT) Bristol strain N2. The *C. briggsae* strain AF16 (Fodor et al., 1983) was used where appropriate. Worm manipulations were performed as previously described (Sulston and Hodgkin, 1988). For microscopy, worms were mounted on slides with thin pads of 2% agarose melted in 0.5% 1-phenoxy 2-propanol (Sigma) in M9 buffer. Animals were picked to a small drop of 0.2% 1-phenoxy 2-propanol on the pad and covered with an 18×18 mm coverslip. Worms were visualised using a Zeiss Axiophot microscope fitted with DIC optics. Supplementary Table 1 describes all strains used in this study.

Sequence comparisons

The *C. briggsae* protein identified on Wormbase (http://www.wormbase.org/) by BlastP, as the nearest homologue of *mab-9* is CBP12816, the product of *CBG24273*. Aligned sequences consisted of 5′ sequence (5.5 kb for *mab-9*, 4.3 kb for CBG24273), plus entire protein coding sequence. We also included 1 kb of downstream sequence in the alignment. Alignments were performed by Pairwise Blast (http://www.ncbi.nlm.nih.gov/blast/bl2seq/wblast2.cgi) using default parameters. Conserved sequences (CNEs) of 25 bp or greater were selected for analysis. Blast alignment of potential regulatory elements was confirmed by means of the Sockeye genomics application (www.bcgsc.bc.ca/sockeye) (Montgomery et al., 2004).

Transgenic animals

Injections were performed in *C. briggsae* or *C. elegans*, using 2–20 ng/μl DNA, as previously described (Mello and Fire, 1995) along with the dominant injection marker *rol-6* (50–100 ng/μl). Transformants were selected on the basis of the dominant *rol-6* phenotype and allowed to self. Stable transmitting lines were examined at the F3 generation or later by epifluorescence and DIC microscopy. Several transgenic lines were examined for each construct and a representative of each is described in this report. Where appropriate, transgenic arrays were integrated using gamma irradiation (Evans, 2006). The integrated *mab-9::gfp* strain *mab-9(e2410); him-8(e1489); eIs34[eEx85(mab-9::GFP+rol-6)]* has been previously described (Woollard and Hodgkin, 2000).

GFP/RFP reporters and rescuing constructs

A *C. briggsae mab-9* promoter-only GFP reporter construct was generated by means of a PCR method (Hobert, 2002). Template was acquired by the single-worm lysis method (Fay and Bender, 2006). PCR was carried out using oligonucleotide primers designed to include the 5′ regulatory sequence of interest, with the reverse primer having a tag complementary to 21 bp of the standard Fire lab GFP vector polylinker sequence (http://www.addgene.org/Fire_Lab). A GFP PCR product was obtained using primers described by Hobert, 2002, using a Fire lab vector with or without nuclear localisation signal, as required. A nested PCR, using products of the above 2 reactions as template, was then performed to generate a single promoter–GFP fusion, which was gel-purified if necessary before injection. Primers to generate tagged *C. brig-mab-9* promoter: Forward 5′-GCAACCGAAAATCTCTTTATGG-3′, reverse 5′-CGACCTGC AGG-CATGCAAGCTGTCCTCTAGAAGAATTTCAGCAG-3′. Nested PCR forward primer: 5′-ATG-CATCGCCCATTAGAAAAGTGACCATACAG-3′. Transgenic lines described in this study are the *C. briggsae* line *AW244* and the *C. elegans* line *AW245*. The *C. elegans mab-9* promoter-only GFP construct pAW150 was made by PCR amplifying the *mab-9* regulatory region using primers containing a 5′*Pst*I site and 3′*Bam*HI site (Forward 5′-GGAACTGCAGCTCCCATCTAAAAAGAGCCG-3′; reverse 5′-GGCGGATCCCAAAATTTAG-TATCTTATGG-3′) and subcloning into Fire Lab vector *pPD96.04*. The corresponding transgenic line described in this study is AW246. The *dpy-7::rfp* transcriptional fusion *pAW289* was made to confirm the hypodermal identity of cells. 249 bp of *dpy-7* promoter sequence (Gilleard et al., 1997) (−373 to −125) was amplified from genomic DNA (obtained by single-worm lysis) using primers oTB7 and oTB8 (containing *Hin*dIII and *Xba*I tags, respectively) and TA cloned into pCRII-TOPO (Invitrogen). The promoter was subcloned into Multiple Cloning Site (MCS) I of pPD49.26 to give the plasmid *pAW288*. mRFP was amplified from pHK210NLS (a kind gift from Hiroshi Kagoshima) using oTB9 and oTB10 (includes SacI tag) and TA cloned into pCRII-TOPO. mRFP(NLS) was subcloned into the MCSII of *pAW288* to generated the plasmid *pAW289*. Primer sequences were as follows: oTB7 5′-AAGCTTTG ACCTCTCGGGAACAATC-3′, oTB8 5′-TCTAGAAGAA-CAGGGTGTGATAAATGAATTG-3′, oTB9 5′-GCCAAAGGACCCAAAGGTAT-3′, oTB10 5′-GAGCTCGGCGCTCAGTTGGAATTCTT-3′. The corresponding transgenic lines described in this study are *AW247* and *AW255*. To make a minimal promoter construct driving GFP from CNE-DE, the region including CNEs D and E was amplified by standard PCR. Forward and reverse primers included tags corresponding to *Hin*dIII and *Xba*I recognition sites, respectively. Forward primer: 5′-AAGCTTTCTC AGATCATAAACCATTATCT GTG-3′. Reverse primer: 5′-TCTAGAATTGACTAATTATCATCAC ACATTCTT-3′. The PCR product was first TA-cloned into the vector pPCR2.1-Topo (Invitrogen) using the manufacturer's standard protocol. The CNE was then subcloned, using *Hin*dIII and *Xba*I, into the Fire lab minimal promoter vector pPD107.94, to give plasmid *pAW339*. The corresponding transgenic line described in this study is *AW248*. A genomic *Cbr-mab-9* rescuing construct was generated by PCR from *AF16 C. briggsae* worms, using primers to include the upstream regulatory sequence of *CBG24273*, full protein-coding sequence and approximately 1 kb of downstream sequence. Forward primer: 5′-GCAACCGAA AATCTCTTTATGTG-3′. Reverse primer: 5′-TCGGATCTCCATTCATCCTC-3′. The corresponding transgenic line described in this study is *AW249*. The genomic rescuing *mab-9::gfp* construct *pAW118* used in this study has been described previously (Woollard and Hodgkin, 2000). The complete genotypes of transgenic strains are shown in Supplementary Table 1.

Site-directed mutagenesis

Conserved upstream and intronic CNEs were deleted individually from the *mab-9::gfp* rescuing construct *pAW118* by means of the QuikChange site-directed mutagenesis kit (Stratagene, La Jolla, CA). As the full-length rescuing construct is too large for direct mutagenesis (18 kb), mutagenesis was carried out on smaller fragments, with the mutagenised fragments being subcloned back into the *pAW118* plasmid. Successful removal of CNEs was confirmed by PCR and sequencing. Plasmids used in this work are *pAW340* (*mab-9ΔCNE-D::gfp*), *pAW341* (*mab-9ΔCNE-E::gfp*) and *pAW342* (*mab-9ΔCNE-DE::gfp*). Transgenic strains generated are *AW250* (*mab-9(e2410)*; *him-8(e1489)*; *ouEx82[mab-9ΔCNE-D::gfp+rol-6]*), *AW251* (*mab-9(e2410)*; *him-8(e1489)*; *ouEx83 [mab-9ΔCNE-E::gfp+rol-6]*, *AW252* (*mab-9(e2410)*; *him-8* (*e1489)*; *ouEx84[mab-9ΔCNE-DE::gfp+rol-6]*) and *AW253* (*mab-9(e2410)*; *him-8(e1489)*; *ouEx85[mab-9ΔCNE-DE::gfp+rol-6+pdpy-7::rfp]*). Transgenic array *ouEx84[mab-9ΔCNE-DE::gfp+ rol-6]* was integrated to give the strain *AW254* (*mab-9(e2410)*; *him-8(e1489)*; *ouIs1 (ouEx84)*).

Dye-filling assay

Mixed staged worms were washed from seeded NGM plates in sterile water. Following 3 washes in water, followed by brief centrifugation, animals were incubated at 20 °C for 30 min in a solution of 10 μg μl^{-1} DiI (1,1′-Dioctadecyl-3,3,3′,3′-tetramethylindocarbocyanine perchlorate) in water. To allow clearing of DiI from the gut, worms were washed briefly in water and transferred to seeded NGM plates for at least 60 min (Shaham, 2006). Animals were mounted for microscopy and examined by epifluorescence.

Lectin staining

Worms were stained with a variety of conjugated lectins, as described previously (Gravato-Nobre et al., 2005). Briefly; adult worms were picked to 1 ml of PBS-T (phosphate-buffered saline containing 0.5% Triton X-100) and washed twice for 5 min. The supernatant was removed and the worms incubated in approximately 30 μl of 50 μg μl^{-1} fluorescein-conjugated lectin for 45 min at 25 °C. Excess lectin was removed by washing 3 times in PBS-T. Worms were mounted for microscopy as described above and examined.

Growth on M. nematophilum

To assess sensitivity of worm strains to infection by *M. nematophilum*, worms were grown on NGM plates seeded with lawns of 10% *M. nematophilum*: 90% OP50 (for brood size assays) or 100% *M. nematophilum* for colonisation assays (Hodgkin et al., 2000). Worms were picked at the L4 stage and allowed to grow at 25 °C. Brood sizes were assessed by counting all viable progeny.

Syto13 staining

Adult hermaphrodite worms grown in the presence of *M. nematophilum* were washed 3 times with TBS and incubated for 1 h at room temperature. Worms were incubated for 1 h in 10 μM Styo13 (Molecular Probes), followed by 3 washes in TBS (Hodgkin et al., 2000).

Results

C. briggsae CBG24273 is a probable orthologue of mab-9

The *C. briggsae* gene predicted by Wormbase to be the closest match to *mab-9* is *CBG24273*. In order to test whether *CBG24273* is

a *bona fide mab-9* orthologue we first analysed the expression of *CBG24273* using a promoter only GFP construct injected into both *C. elegans* and *C. briggsae* (Fig. 1). In *C. elegans*, the expression patterns of the transcriptional *mab-9*::*gfp* (*pAW150*) and *Cbr-mab-9*::*gfp* reporters are very similar to that of the translational fusion *pAW118*, except that B and F expression of the *C. briggsae* GFP reporter was never observed in *C. elegans*, even though posterior hypodermal expression was robust (Fig. 1A). Expression of the same reporter construct in *C. briggsae* was observed at lower intensities than in *C. elegans* and tended to be more mosaic, especially in adult worms; however we were able to observe GFP in nuclei of the ventral nerve cord (VNC) and in the posterior hypodermis (Fig. 1B).

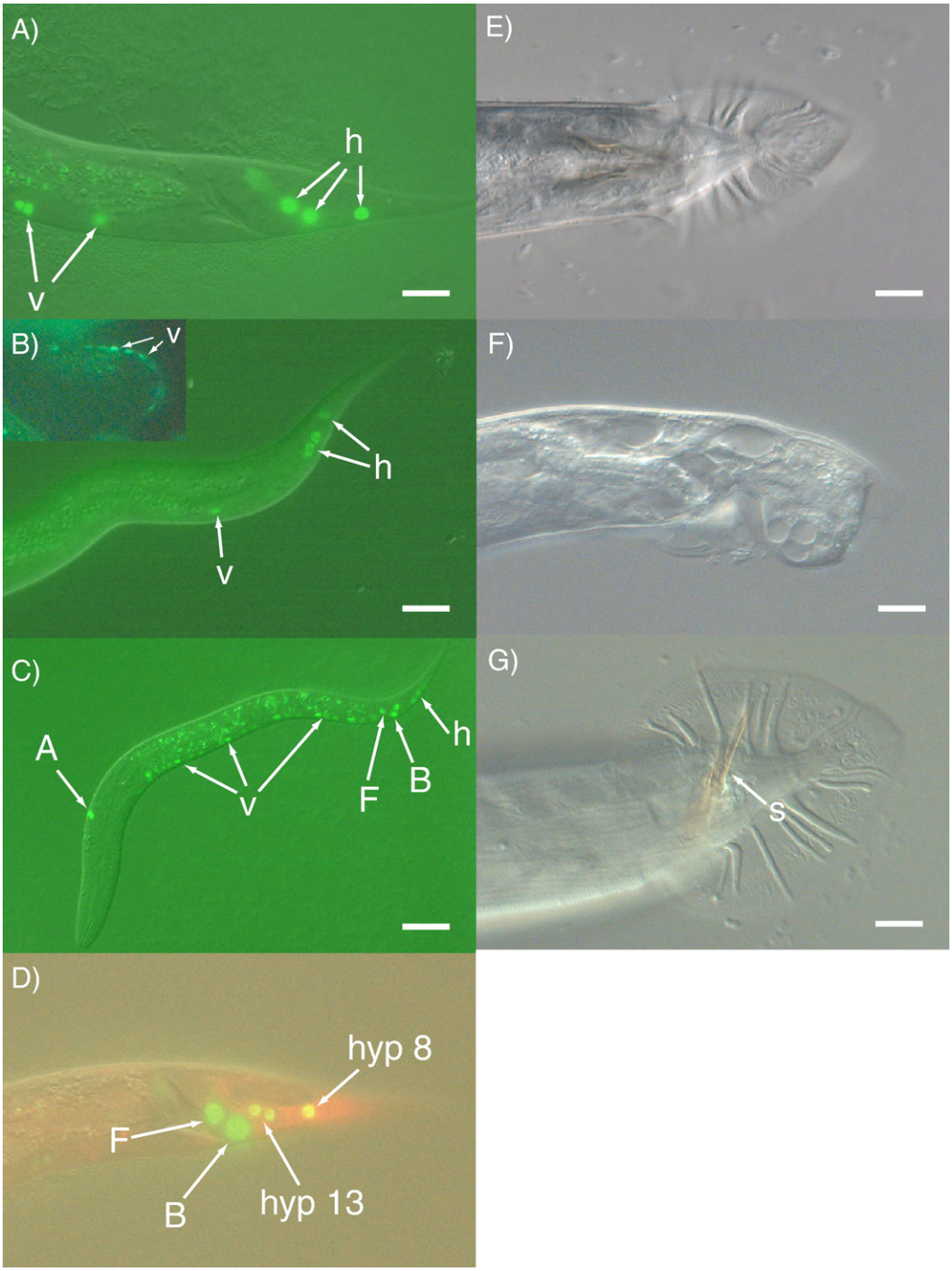

Fig. 1. *C. briggsae CBG24273* is a probable orthologue of *mab-9*. (A) L4 animal of *C. elegans* strain *AW245*, expressing a *Cbr-mab-9* promoter-only GFP fusion. GFP expression was observed in posterior hypodermal nuclei (h) and nuclei of the ventral nerve cord (VNC) (v) but not in panels B or F. (B) L4 animal of *C. briggsae* strain *AW244*, expressing the same construct. GFP expression was observed in a similar pattern. Inset is a developing 3-fold embryo showing brighter VNC expression. (C) *C. elegans CB5481* animal showing WT MAB-9::GFP expression in VNC neurons (v), the ALA head neuron (A), F and B nuclei (F, B respectively) and hypodermal nuclei (h). (D) *C. elegans* strain *AW255*, L4 worm, expressing a *Cel-mab-9* promoter only GFP fusion. This reporter expresses in the tail in a similar manner to the genomic construct *pAW118*, being observed in panels B and F nuclei, two nuclei of the hyp7 syncytium (hermaphrodites) or hyp13 (males, as pictured) and a hyp8 nucleus (labelled). The identity of hypodermal cells is confirmed by colocalisation with a hypodermal-specific DPY-7::RFP transcriptional fusion. (E) WT male tail. (F) *mab-9(e2410)* male. Failure of the panels B and F lineage leads to severe disruption of tail development and grossly abnormal structures. (G) Adult male of strain *AW249* showing full rescue of all male tail defects by full length *Cbr-mab-9*. Normal male tail structures including spicules (s) and fan are present. Scale bar: 10 μm. Posterior is to the right in all panels.

Once again, it was not possible to demonstrate B or F expression of this reporter in *C. briggsae*.

Given this difference in observable expression pattern between *C. elegans* and *C. briggsae* promoter-only fusions and the fact that B and F cells are major sites of MAB-9 function, we next tested whether a genomic clone of *CBG24273* was capable of rescuing *C. elegans mab-9* mutants. At least 5 independent lines were obtained, all of which displayed complete phenotypic rescue (Fig. 1G). Therefore, it seems likely that our failure to detect B and F expression of *Cbr-mab-9*::*gfp* in either *C. elegans* or *C. briggsae* is due to expression being below some threshold level in these cells, rather than pointing to a potential functional difference between the two genes. We cannot rule out the possibility, however, that there could be some cell-nonautonomous mechanism (from cells that express *mab-9*) influencing B and F development. Overall, these data indicate that *CBG24273* is a probable orthologue of *C. elegans mab-9*. We henceforward refer to *CBG24273* as *Cbr-mab-9*.

CNEs in mab-9

We initially performed a comparison of the putative regulatory regions of *mab-9* and *Cbr-mab-9* by means of a pairwise Blastn search using the default parameters. For *mab-9*, we used 5.5 kb of upstream sequence (which has previously been shown to be required for complete rescue of the *mab-9* phenotype; Woollard and Hodgkin, 2000), the entire ORF and 1 kb of downstream sequence. For *Cbr-mab-9*, we used homologous sequence, with the exception that the upstream sequence extended only 4.3 kb past the transcription start site (this is the extent of the current available sequence). As this amount of upstream sequence completely rescues all aspects of the *mab-9* phenotype, we think it unlikely that we missed important regulatory elements in our analysis. Unsurprisingly, protein-coding sequences are well conserved between *C. elegans* and *C. briggsae mab-9*, whereas most of the non-coding sequence is poorly conserved. However, we identified 5 blocks of conserved sequence (CNEs) in the upstream regulatory region, ranging between 27 and 51 bp in length; these we have termed CNE-A to CNE-E (Fig. 2). All the CNEs are in the same orientation and relative position in *C. elegans* and *C. briggsae*, although the distance spanning these CNEs in *C. briggsae* is somewhat smaller than in *C. elegans* (2948 bp from the start of CNE-A to the start of CNE-E in *C. briggsae*, compared with 3943 bp in *C. elegans*) (Fig. 2A). A sixth CNE, CNE-F (actually comprising 2 blocks of very close sequence similarity separated by a short stretch of divergent sequence) was discovered in the third intron. Although these stretches of high sequence identity were originally identified by means of Pairwise Blast alignment, conservation of the 6 regions between *C. elegans* and *C. briggsae* was subsequently confirmed using the Sockeye comparative genomics visualisation application.

CNE-D/E is required for expression of mab-9 in the posterior hypodermis

To establish which, if any, of the CNEs are required for normal *mab-9* expression in *C. elegans*, we deleted each of these from the rescuing construct by site-directed mutagenesis. Transgenic animals were then generated containing these deletions and examined for changes in the GFP expression pattern. Transgenic worms carrying *pAW340* (*mab-9ΔCNE-D*::*gfp*) or *pAW341* (*mab-9ΔCNE-E*::*gfp*) display normal expression of MAB-9::GFP in the nervous system and B and F cells.

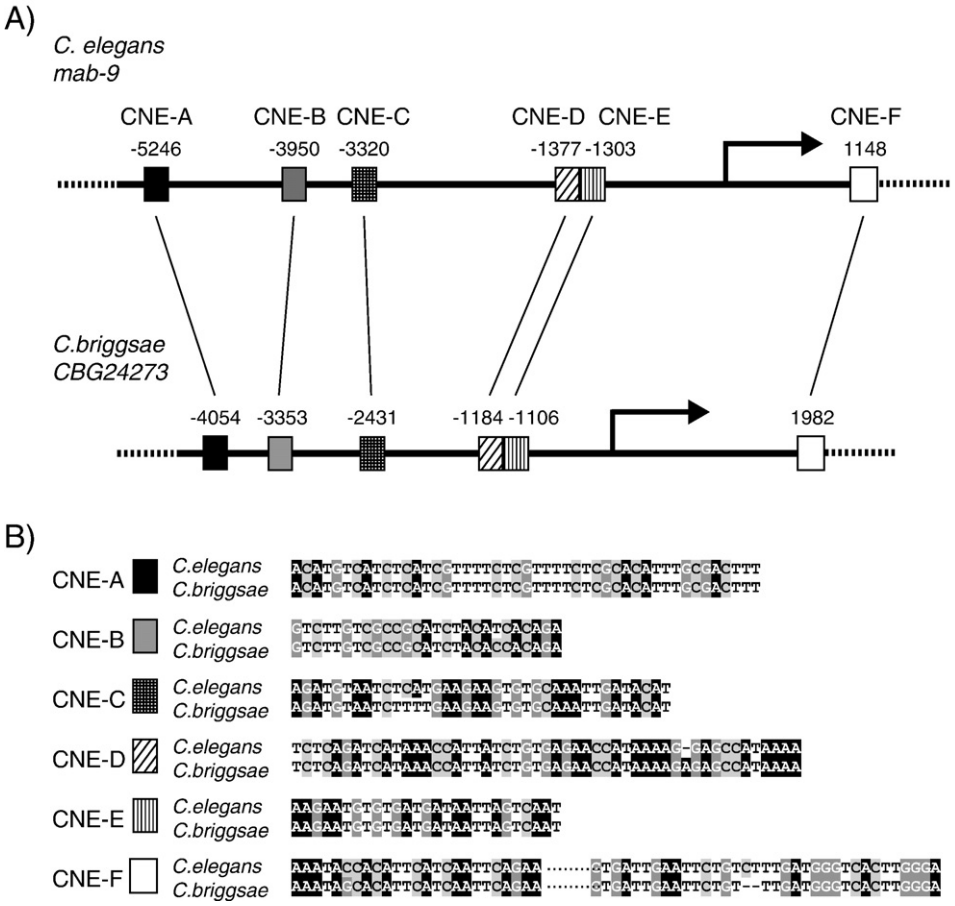

Fig. 2. Alignment of *mab-9* and *CBG24273* regulatory regions. (A) Cartoon showing conserved order and spacing of CNEs A–F. Arrow denotes transcriptional start site. CNE-D and CNE-E are adjacent to one another and are treated as on element, CNE-DE for much of this study. (B) Alignments of each CNE A–F between *C. elegans* and *C. briggsae*.

However, both deletion constructs show reduced GFP expression in the posterior hypodermis (data not shown). A double-deletion was therefore made, lacking both of these conserved elements, *pAW342* (*mab-9ΔCNE-DE::gfp*). Transgenic animals carrying this construct were found to completely lack tail hypodermal expression in all cases in both males and hermaphrodites (Fig. 3B), although all other elements of the *mab-9* expression pattern (including B and F expression) were normal. Failure of MAB-9::GFP expression in posterior hypodermal cells does not appear to be the result of a change in cell identity as they still express the p*dpy-7::rfp* hypodermal marker when this is co-injected with the other plasmids (Fig. 3B). Deletion analysis of the 4 other CNEs, either singly or in various combinations, revealed no obvious changes in expression pattern (data not shown).

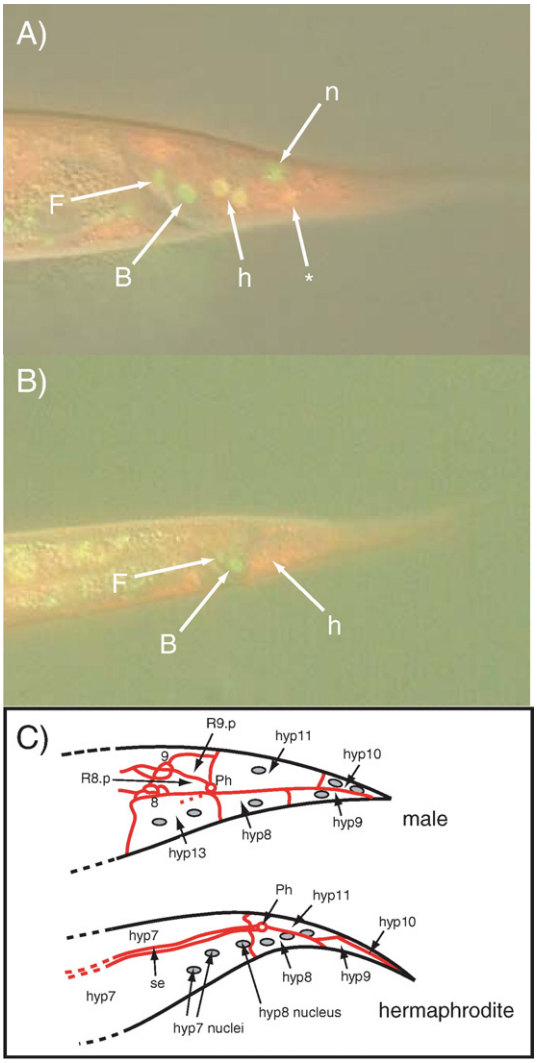

Fig. 3. CNE-DE is essential for posterior hypodermal expression of MAB-9::GFP. (A) strain *AW247* L4 hermaphrodite, expressing full length *Cel-mab-9::gfp* and *dpy-7::rfp*. F and B cells have a non-hypodermal identity and nuclei appear green (labelled F, B). Posterior hypodermal cells co-express both MAB-9::GFP and DPY-7::RFP and nuclei appear yellow. These hypodermal nuclei correspond to two hyp 7 nuclei (h) and a hyp 8 nucleus (asterisk) just out of the plane of focus. n=tail neuron. (B) Strain *AW253* L4 hermaphrodite, expressing the *mab-9ΔCNE-DE::gfp* construct and *dpy-7::rfp* in a *mab-9(e2410)* mutant background. No MAB-9::GFP is visible in the posterior hypodermis. Posterior hypodermal cells (h) retain their identity as shown by expression of the hypodermal marker DPY-7::RFP and appear red. All other components of the *mab-9* expression pattern are observed, but are outside the plane of this photomicrograph. (C) Simplified illustration of tail hypodermal compartments prior to tail tip retraction in male and in late L4 hermaphrodite (after Nguyen et al., 1999). Ph=phasmid, se=lateral seam hypodermis.

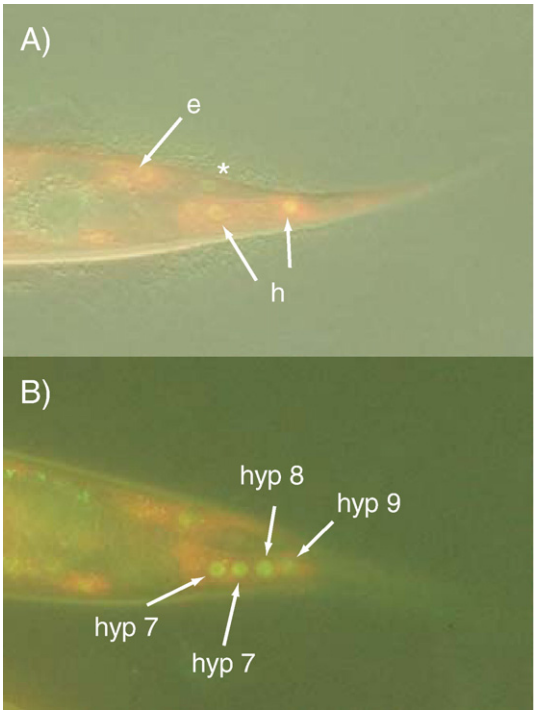

Fig. 4. CNE-DE drives expression of a GFP reporter in the posterior hypodermis. (A, B) Animals carrying the *pAW339* CNE-DE driven minimal promoter construct (Strain *AW248*). Expression of the CNE-DE driven GFP reporter is seen in posterior hypodermal nuclei co-localised with DPY-7::RFP (h). Ectopic expression of CNE-DE driven GFP is observed in some other more anterior hypodermal cells (e). One such cell is shown exhibiting mosaicism of the DPY-7::RFP marker (asterisk). In B: 4 hypodermal nuclei (2 hyp 7, hyp 8 and hyp 9 nuclei) are seen co-expressing CNE-DE driven GFP and DPY-7::RFP.

CNE-DE is sufficient to drive expression of mab-9 in the posterior hypodermis

A minimal promoter construct, *pAW339*, was designed to test whether CNE-DE is sufficient to drive expression of a GFP reporter *in vivo*. Transgenic animals carrying this construct did indeed express GFP in cells of the posterior hypodermis (Fig. 4), as confirmed by the co-localisation of the GFP with p*dpy-7::*RFP in hyp7, hyp8 and hyp9 nuclei. We also noted some expression of GFP in more anterior hypodermal cells (but nowhere else in the worm), suggesting that the endogenous regulatory region of *mab-9* may contain transcription factor binding sites that are normally bound by repressors to prevent strong expression of MAB-9 in the anterior syncytial hypodermis.

Ablation of posterior hypodermal expression of mab-9 results in defects in male tail morphogenesis

Given the lack of hypodermal expression of *mab-9* in reporter constructs lacking CNE-DE, we were interested to see whether this change in expression pattern is correlated with phenotypic effects. Transgenic animals were therefore generated carrying the *mab-9ΔCNE-DE::gfp* construct in a *mab-9* mutant background. These males display rescue of the gross internal tail defects associated with the function of MAB-9 in the B and F blast cells (Fig. 5) (defective or absent spicules, for example), but harbour a number of more subtle tail defects, including the appearance of bulges near the bases of the rays, increased fusion of rays 8 and 9 and abnormal tail tips (Fig. 5, Table 1). Importantly, the same male tail defects were observed in integrated as well as extrachromosomal lines, indicating that they were not a consequence of mosaic expression of the mutagenised rescuing construct (The data shown in Fig. 5 is derived from the integrated strain *mab-9(e2410)*; *him-8(e1489)*; *ouIs1[ouEx84 (mab-*

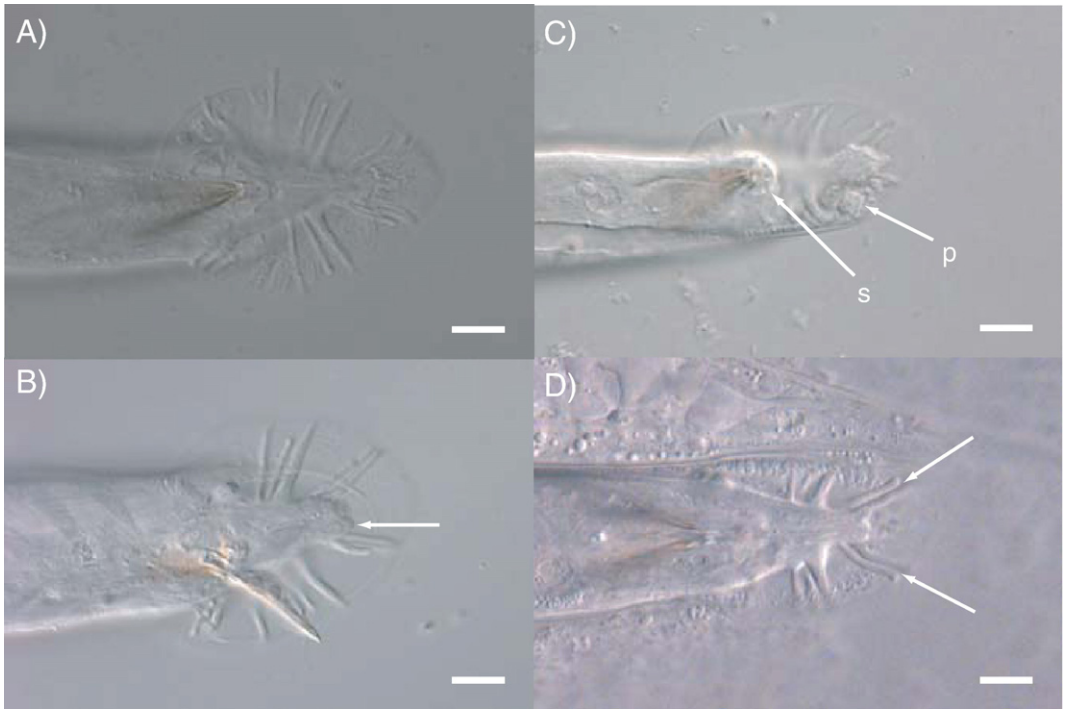

Fig. 5. Male tail defects associated with lack of hypodermal MAB-9 expression. (A) Strain *CB5481* adult male, expressing full length integrated *mab-9::GFP* in a *mab-9* mutant background, showing WT appearance. (B–D): *AW254* adult males, expressing an integrated *mab-9ΔCNE-DE::gfp* construct. Various defects are evident. (B) Abnormal tail tip (arrow). (C) blobby protrusions (p) and swollen bursa (s). (D) fused rays 8 and 9 (arrow). Scale bar: 10 μm.

9ΔCNE-DE::gfp+rol-6)] (Strain *AW254*). Such defects are never observed in *mab-9* males rescued with the WT genomic construct *pAW118*. The tail tip defect is suggestive of a partial failure in tail tip retraction, but could also be explained by blebbing out of another tissue, like hyp13 or the phasmids. Since the tail tip abnormalities are situated in close proximity to the phasmid openings, we performed dye-filling assays on male and hermaphrodite worms of all life cycle stages in order to determine if there is a defect in dye-filling. In all worms stained, dye filling appeared normal (data not shown), indicating that the phasmids are functioning, although not ruling out the possibility of a morphogenetic defect to phasmid tissue affecting tail tip morphogenesis.

Wild-type male tail fans are cuticular structures and contain modifications to the cuticle which include tanning of the posterior-most part of the fan between the two opposing 9th rays (Link et al., 1988). Normally this tanning is visible in the form of autofluorescence, which can be observed under epi-fluorescence using standard FITC filters (Fig. 6). *mab-9*(*e2410*) males typically lack a normal fan structure and do not exhibit this autofluorescence (Fig. 6B), whereas fan autofluorescence of *mab-9* male tails rescued with the WT genomic construct *pAW118* is normal (Fig. 6C). *mab-9* males carrying the CNE-DE deletion exhibit an altered pattern of autofluorescence (Fig. 6D, Table 1), suggesting a function for MAB-9 in posterior hypodermal cells in regulating gene(s) responsible for the correct processing and/or secretion of male tail collagens.

Changes in lectin binding properties have previously been reported in worms both with observable male-tail defects and also those that otherwise appear grossly wild-type (Link et al., 1992). Since the altered tail autofluorescence is highly suggestive of a defect in tail cuticle processing leading to altered surface properties, we performed lectin staining with the Jack Bean lectin, Concanavalin A (ConA) to identify any changes in cuticle carbohydrate recognition. Staining in WT or fully rescued *mab-9* mutant males (transgenic for *pAW118*) was restricted to the region immediately surrounding the cloaca and the openings of the phasmids, if seen at all (Figs. 6E and G). *mab-9* males carrying the CNE-DE deletion, however, exhibited ConA staining at the edge of the cuticular fan in almost all individuals examined (Fig. 6H). Completely un-rescued *mab-9* males also display strong lectin staining at the fan edge, where present (*mab-9* mutants often lack a proper fan all together), along

Table 1
Male tail abnormalities in worms lacking hypodermal MAB-9 expression

	him-8(e1489)	mab-9(e2410); him-8(e1489)	mab-9(e2410); him-8(e1489); eIs34(eEx85[mab-9::gfp+rol-6]) (CB5481)	mab-9(e2410); him-8(e1489); ouIs1(ouEx84 [mab-9ΔCNE-DE::gfp+rol-6]) (AW254)
Percentage males with fused rays 8/9	14% (n=78)	N/D[a]	12% (n=84)	52% (n=113)[b]
Percentage males with aberrant, reduced or absent tail autofluorescence	6.9% (n=58)	100% (n=50)[c]	14.8% (n=54)	74.5% (n=51)

[a] ND=not determined. *mab-9*(*e2410*) males were not scored for ray fusion as posterior structures are typically too severely disrupted for this to be assessed.
[b] This is a conservative estimate as a small percentage of worms exhibit tail protrusions that can mask the fused-ray phenotype. These protrusions were never observed in *him-8* (e1489) worms.
[c] Tail fan autofluorescence was absent in all worms examined. As the *mab-9* phenotype often results in very severe tail abnormalities, this figure represents the absence of autofluorescence in male worms where a discernible fan could be seen.

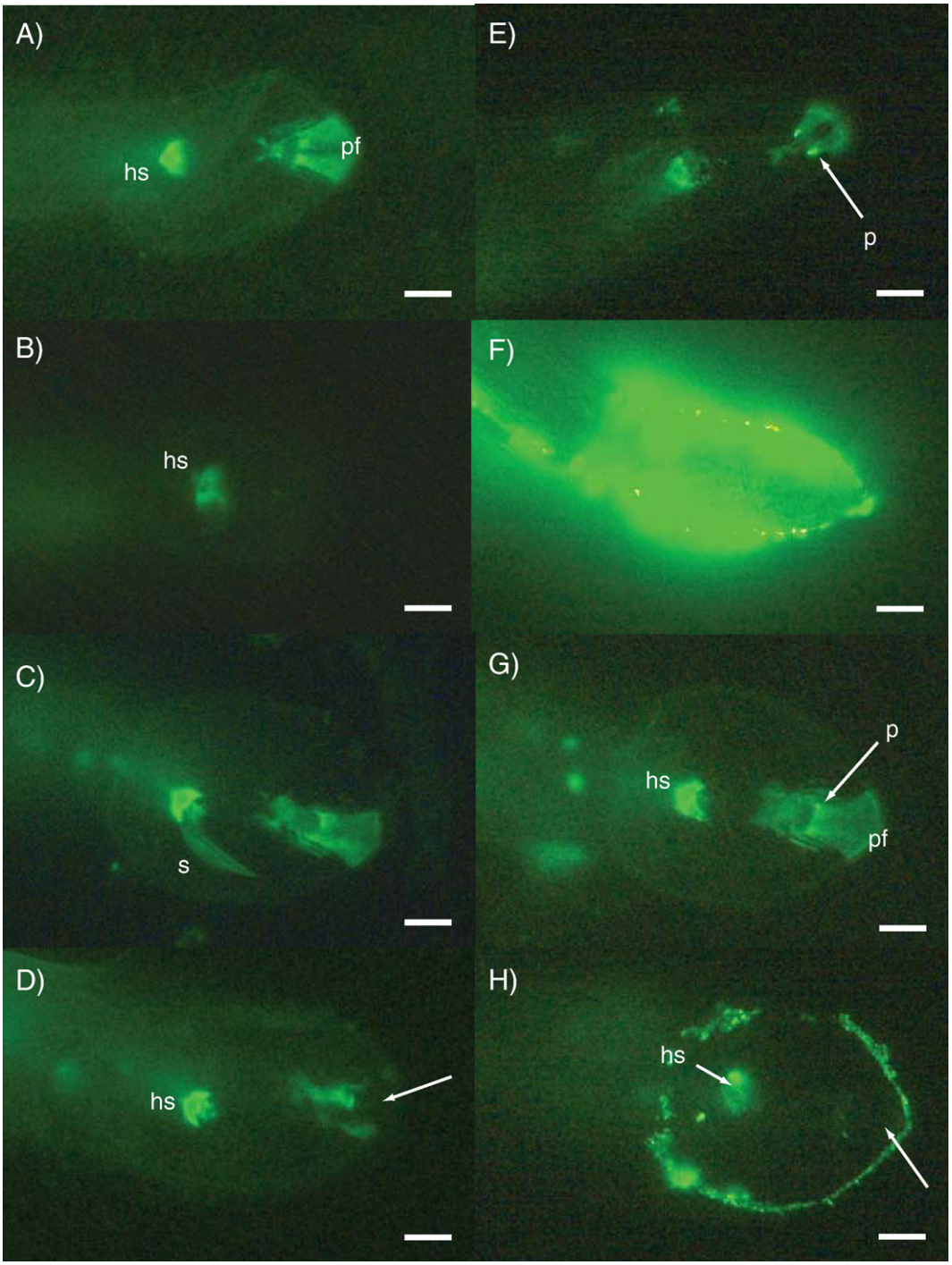

Fig. 6. Male tail cuticle defects associated with lack of hypodermal MAB-9 expression. (A) *him-8(e1489)* adult male showing the characteristic autofluorescence of the WT male tail fan. The hook sensilum (hs) and posterior fan (pf) are strongly autofluorescent, the latter in a characteristic (fan-shaped) pattern. (B) *mab-9(e2410); him-8(e1489)* male tail autofluorescence; posterior fan fluorescence is completely absent although some autofluorescence is still associated with the hook sensillum (hs). (C) *CB5481* rescued male, expressing full length integrated *mab-9::GFP* in a *mab-9* mutant background, showing WT tail autofluorescence. Spicules (s) are everted in this individual. (D) *AW254* male, expressing an integrated *mab-9ΔCNE-DE::gfp* construct, lacking MAB-9 expression in the posterior hypodermis. Posterior fan autofluorescence is greatly reduced or absent, or is aberrant (as in this individual). Arrow points to portion of the tail where autofluorescence is lacking. (E–H) Male tails stained with FITC-ConA. E: *him-8(e1489)* male showing WT ConA staining. Posterior fan autofluorescence can be observed, as can lectin staining of phasmid openings (p). (F) *mab-9(e2410)*; *him-8(e1489)* male tail. Very strong staining is observed in these mutants, extending anteriorly from the tail for up to one-third of the length of the worm. (G) *CB5481* rescued male showing restoration of normal cuticle properties. Posterior fan (pf) autofluorescence can be observed, as can small foci of lectin binding at the phasmid openings (p). (H) *AW254* male lacking MAB-9 expression in the posterior hypodermis. Abnormal lectin binding is observed; the edge of the fan is strongly stained with FITC-conjugated ConA. Tail tip autofluorescence is absent (arrow). Scale bar: 10 μm.

with bright localisation of the lectin to the posterior cuticle of the worm, for up to 1/3 of the length of the animal (Fig. 6F). We therefore suggest that it is the loss of *mab-9* expression specifically in the posterior hypodermis that results in this cuticle secretion/modification defect.

Ablation of posterior hypodermal mab-9 expression results in reduced sensitivity to infection by M. nematophilum

Changes in cuticle properties in worms lacking posterior hypodermal expression of *mab-9* may result in an altered response

to bacterial infection. We therefore tested the response of animals lacking posterior hypodermal expression of MAB-9 to infection with the *C. elegans* pathogenic bacterium *M. nematophilum* which adheres to the cuticle overlying such hypodermal cells (Hodgkin et al., 2000). We found that these animals display a reduced sensitivity to infection; firstly, we measured brood sizes of infected animals and

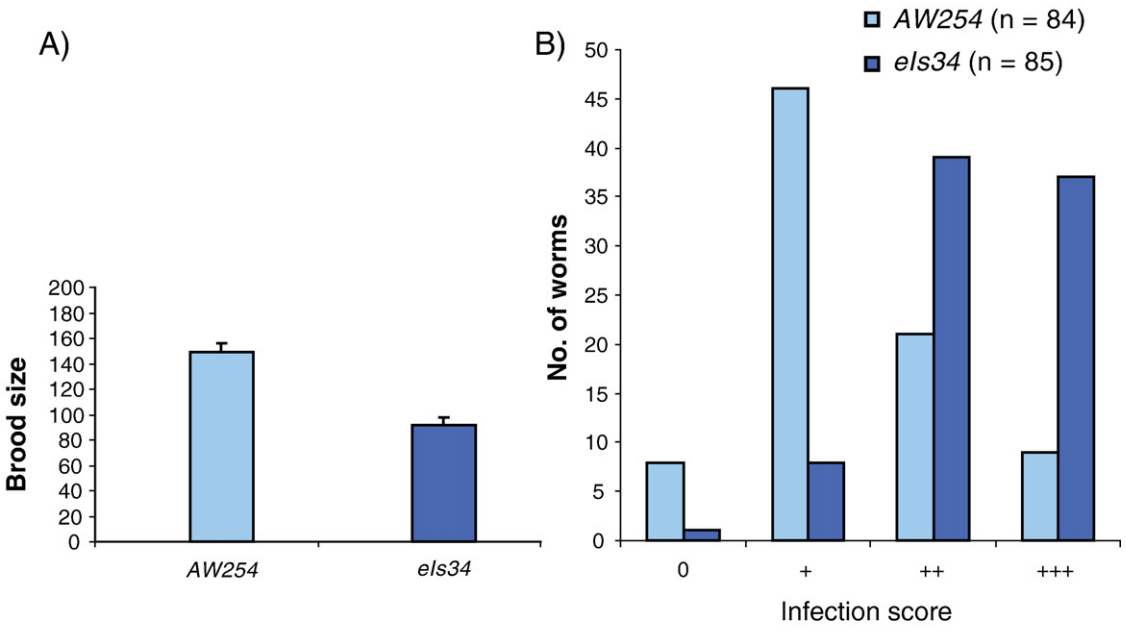

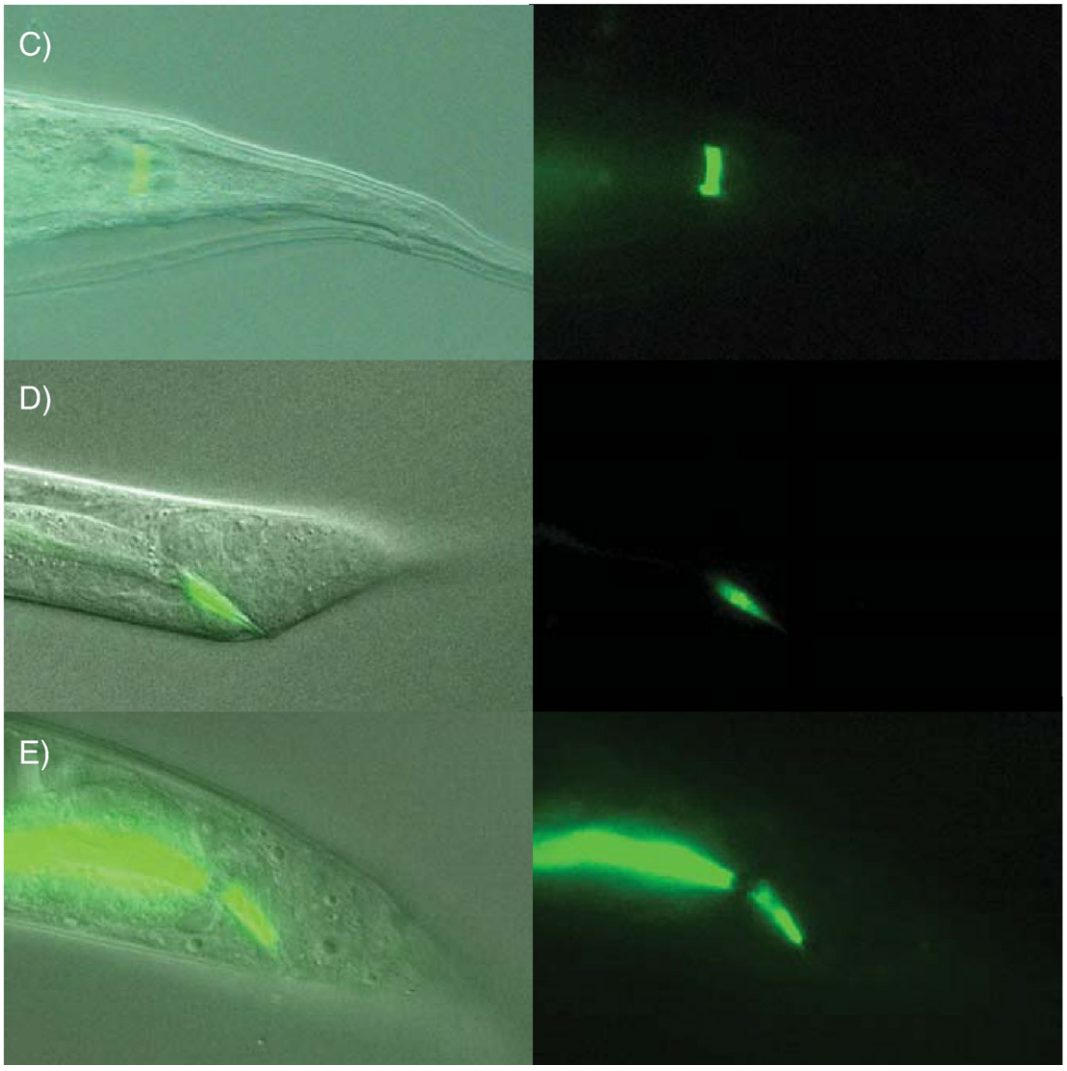

found that worms expressing MAB-9 in posterior hypodermal cells had a lower average brood size than worms lacking posterior hypodermal MAB-9 expression (Fig. 7A). Growth on pure cultures of OP50 on the other hand, led to no observable differences between these two worm strains (data not shown). Next, we used the vital dye Syto13 to stain for the presence of infecting bacteria colonising the rectum and peri-anal region of worms grown on lawns of 100% *M. nematophilum*. As indicated in Fig. 7B, the overall severity of infection with *M. nematophilum* is reduced in worms lacking posterior hypodermal MAB-9 expression, as evidenced by a reduced colonisation of the rectum and perianal region by bacteria.

Discussion

We have identified 6 CNEs in the regulatory region of *mab-9* and have demonstrated a co-operative role for two of them (CNE-DE) in the expression of MAB-9 in posterior hypodermal cells. Loss of posterior hypodermal expression of MAB-9 correlates with various hypodermal defects in both males and hermaphrodites which appear to stem from incorrect cuticle secretion and/or processing. We have shown that CNE-DE is both necessary and sufficient for expression of MAB-9 in the posterior hypodermis, suggesting that the transcription factor(s) that binds them is solely responsible for this aspect of *mab-9* expression *in vivo*. "Modular" promoters have been previously described (Wenick and Hobert, 2004), in which different promoter elements are responsible for various components of gene expression.

This is the first demonstration of a role for MAB-9 outside of the rectal epithelium and nervous system. Tail defects such as those observed in animals carrying our CNE deletion are not observable in other existing *mab-9* alleles because they are masked by the gross loss of internal structures characteristic of these mutants. The CNE-DE deletion construct in *mab-9* mutants is therefore acting as an informative hypomorph. Mutants with tail tip defects have been reported elsewhere. Generally these result from failure of cytoplasmic retraction and typically have pointed (leptoderan) tail morphologies (Del Rio-Albrechtsen et al., 2006). The defects we observe in the CNE-DE deletion hypomorph is less severe than this but presumably results from incorrect function of posterior hypodermal cells.

The altered tail autofluorescence observed in *mab-9* null alleles and in the hypomorph suggests that cuticle processing and/or secretion is abnormal in these worms. Consistent with this suggestion is our finding that these males also display abnormal lectin binding properties when stained with FITC-conjugated ConA. Lectin binding abnormalities have been observed in worms that are grossly WT, such as some *srf* mutants (Link et al., 1992) and sensory ray mutants (Ko and Chow, 2000), as well as in males with more severe copulatory bursa defects (Link et al., 1988). Lectins have been studied in a wide range of biological systems and have documented roles in both cell–cell and cell–molecule interactions (reviewed in Sharon and Lis, 2004). Of particular relevance to this study is the fact that surface carbohydrate recognition by pathogens can be mediated by lectins. We find reduced sensitivity to *M. nematophilum* infection in *mab-9* mutants carrying the CNE-DE deletion construct, caused by reduced colonisation of the rectum. Previous studies have shown that multiple genes are involved in the processes of infection by *M. nematophilum* and the subsequent tail-swelling response (Gravato-Nobre et al., 2005). For example, *srf-3*, a nucleotide sugar transporter expressed in seam cells, is required for bacterial adherence to the cuticle by *M. nematophilum* (Höflich et al., 2004) and several Bus (Bacterially Unswollen) mutants display altered cuticle properties (Gravato-Nobre et al., 2005). The results from our present study suggest that the loss of MAB-9 expression in the posterior hypodermis leads to alteration or reduction of bacterial adherence molecules culminating in less severe infection and that this may be reflected in altered lectin binding properties in the tail cuticle.

The posterior hypodermal nuclei that fail to express MAB-9::GFP when CNE-DE is deleted include 2 nuclei that constitute the male-specific compartment hyp13 (Nguyen et al., 1999). In hermaphrodites these nuclei fuse with other hypodermal nuclei to form part of the hyp7 syncytium, whereas in males they form a separate compartment, fusing with hyp7 only at late L4. The function of the hyp13 compartment is unclear at present. The data presented here suggest that hyp13, perhaps acting together with hyp8 and/or hyp9, may have a role in the secretion and/or processing of male-specific collagens. It is also possible that MAB-9 is acting non-autonomously in the posterior hypodermis to affect the properties of hyp13-neighbouring cells. It is unclear from our data whether MAB-9 acts to correctly specify the fate of these hypodermal cells, or is involved in some downstream function. We still observe DPY-7::RFP expression in all posterior hypodermal cells in *mab-9* mutants, indicating that they still have overall hypodermal identity, but our experiments do not rule out more subtle cell fate defects.

The sequencing of the *C. briggsae* genome has provided a useful resource for comparative genomics and has enabled identification of *cis*-regulatory sequences in several genes. For example, a dissection of the regulatory elements controlling *egl-5* expression identified 20 conserved elements, which, with the exception of two elements, were conserved both in terms of their order and orientation (Teng et al., 2004). The regulatory elements necessary for expression of *dpy-7*, although initially identified by deletion analysis, were found to be conserved in a block of homology between *C. elegans* and *C. briggsae* (Gilleard et al., 1997). *pes-10* minimal promoter constructs generated using promoter sequence conserved between *C. elegans* and *C. briggsae* have also been used to identify *cis*-regulatory elements of genes expressed in vulval cells and the anchor cell (Kirouac and Sternberg, 2003). It is perhaps surprising, therefore, that deletion analysis of the 4 other *mab-9* CNEs, either singly or in various combinations, revealed no obvious changes in expression pattern or rescuing ability. It is very unlikely that *mab-9* and *Cbr-mab-9* are regulated by different transcription factors, given the largely conserved expression pattern, so a more likely explanation would be that enhancers driving expression of MAB-9 in the nervous system and in B and F blast cells are redundant with elements outside of the CNEs, or not present in these conserved blocks at all. As comparative genomic approaches to identifying *cis* regulatory "signatures" become more widespread, it will be interesting to assess whether this experience (2 out of 6 CNEs being found to be important for controlling gene expression) will turn out to be rare, or a more common occurrence. Whatever the outcome, these types of study will provide powerful information about the nature of gene regulatory regions and their evolution.

Fig. 7. Worms lacking posterior hypodermal MAB-9::GFP expression have reduced susceptibility to infection by *M. nematophilum*. (A) Graph showing brood sizes of infected worms. *AW254* worms lacking MAB-9 expression in the posterior hypodermis grown on 10% *M. nematophilum* have larger brood sizes when compared with *CB5481* worms rescued with the WT *mab-9::gfp* transgene. (B) Graph showing severity of infection of worms grown on 100% *M. nematophilum*. *AW254* worms lacking MAB-9 expression in the posterior hypodermis show decreased severity of infection compared with *CB5481* worms when viewed after Syto13 staining. Adult worms were inspected and given a score of 0 to +++ as follows: 0 — bacteria not detected, + colonisation of the peri-anal region only, ++ bacteria observed in rectum, +++ bacteria in rectum and gut. (C–E) Syto13 staining of infected worms showing rationale for scoring. (C) *M. nematophilum* adhering to the peri-anal region (infection score +). (D) colonisation of the rectum (infection score ++). (E) complete colonisation of rectum and gut. Merged DIC/fluorescence images are on the left, fluorescence only on the right.

Acknowledgments

This work was funded by the Medical Research Council (MRC) grant G0001282 to AW. We would like to thank Jonathan Hodgkin for useful discussion, and for providing resources to MGN.

Appendix A. Supplementary data

Supplementary data associated with this article can be found, in the online version, at doi:10.1016/j.ydbio.2008.02.049.

References

Chisholm, A.D., Hodgkin, J., 1989. The mab-9 gene controls the fate of B, the major male-specific blast cell in the tail region of *Caenorhabditis elegans*. Genes Dev. 3, 1413–1423.

Del Rio-Albrechtsen, T., Kiontke, K., Chiou, S.-Y., Fitch, D.H.A., 2006. Novel gain-of-function alleles demonstrate a role for the heterochronic gene lin-41 in *C. elegans* male tail tip morphogenesis. Dev. Biol. 297, 74–86.

Evans, Thomas C., 2006. Transformation and microinjection. The *C. elegans* Research Community. WormBook. doi/10.1895/wormbook.1.108.1, http://www.wormbook.org.

Fay, D., Bender, A., 2006. Genetic mapping and manipulation: Chapter 4—SNPs: introduction and two-point mapping. The *C. elegans* Research Community. WormBook. doi/10.1895/wormbook.1.93.1, http://www.wormbook.org.

Fodor, A., Riddle, D.L., Nelson, F.K., Golden, J.W., 1983. Comparison of a new wild-type *Caenorhabditis briggsae* with laboratory strains of *C. briggsae* and *C. elegans*. Nematologica 29, 203–217.

Gilleard, J.S., Barry, J.D., Johnstone, I.L., 1997. cis regulatory requirements for hypodermal cell-specific expression of the *Caenorhabditis elegans* cuticle collagen gene dpy-7. Mol. Cell. Biol. 17, 2301–2311.

Gravato-Nobre, M.J., Nicholas, H.R., Nijland, R., O'Rourke, D., Whittington, D.E., Yook, K.J., Hodgkin, J., 2005. Multiple genes affect sensitivity of *Caenorhabditis elegans* to the bacterial pathogen *Microbacterium nematophilum*. Genetics 171, 1033–1045.

Hobert, O., 2002. PCR fusion-based approach to create reporter gene constructs for expression analysis in transgenic *C. elegans*. BioTechniques 32, 728–730.

Hodgkin, J., 1983. Male phenotypes and mating efficiency in *Caenorhabditis elegans*. Genetics 103, 43–64.

Hodgkin, J., Kuwabara, P.E., Corneliussen, B., 2000. A novel bacterial pathogen, *Microbacterium nematophilum*, induces morphological change in the nematode *C. elegans*. Curr. Biol. 10, 1615–1618.

Höflich, J., Berninsone, P., Göbel, C., Gravato-Nobre, M.J., Libby, B.J., Darby, C., Politz, S.M., Hodgkin, J., Hirschberg, C.B., Baumeister, R., 2004. Loss of srf-3-encoded nucleotide sugar transporter activity in *Caenorhabditis elegans* alters surface antigenicity and prevents bacterial adherence. J. Biol. Chem. 279, 30440–30448.

Huang, X., Cheng, H.-J., Tessier-Lavigne, M., Jin, Y., 2002. MAX-1, a novel PH/MyTH4/FERM domain cytoplasmic protein implicated in netrin-mediated axon repulsion. Neuron 54, 563–576.

Kirouac, M., Sternberg, P.W., 2003. cis-regulatory control of three cell fate-specific genes in vulval organogenesis of *Caenorhabditis elegans* and *C. briggsae*. Dev. Biol. 257, 85–103.

Ko, F.C.F., Chow, K.L., 2000. Mutations with sensory ray defect unmask cuticular glycoprotein antigens in *Caenorhabditis elegans* male tail. Dev. Growth Differ. 42, 69–77.

Link, C.D., Ehrenfels, C.W., Wood, W.B., 1988. Mutant expression of male copulatory bursa surface markers in *Caenorhabditis elegans*. Development 103, 485–495.

Link, C.D., Silverman, M.A., Breen, M., Watt, K.E., Dames, S.A., 1992. Characterization of *Caenorhabditis elegans* lectin-binding mutants. Genetics 131, 867–881.

Mello, C., Fire, A., 1995. DNA transformation. Methods Cell Biol. 48, 451–482.

Montgomery, S.B., Astakhova, T., Bilenky, M., Birney, E., Fu, T., Hassel, M., Melsopp, C., Rak, M., Robertson, A.G., Sleumer, M., Siddiqui, A.S., Jones, S.J.M., 2004. Sockeye: a 3D environment for comparative genomics. Genome Res. 14, 956–962.

Nguyen, C.Q., Hall, D.H., Yang, Y., Fitch, D.H.A., 1999. Morphogenesis of the *Caenorhabditis elegans* male tail tip. Dev. Biol. 207, 86–106.

Packham, E.A., Brook, J.D., 2003. T-box genes in human disorders. Hum. Mol. Genet. 12, R37–R44.

Papaioannou, V.E., 2001. T-box genes in development: from hydra to humans. Int. Rev. Cytol. 207, 1–70.

Seydoux, G., Fire, A., 1994. Soma-germline asymmetry in the distributions of embryonic RNAs in *Caenorhabditis elegans*. Development 120, 2823–2834.

Shaham, S., 2006. Methods in cell biology. The *C. elegans* Research Community. WormBook. doi/10.1895/wormbook.1.49.1, http://www.wormbook.org.

Sharon, N., Lis, H., 2004. History of lectins: from hemagglutinins to biological recognition molecules. Glycobiology 14, 53R–62R.

Sulston, J., Hodgkin, J., 1988. Methods. In: Wood, W.B. (Ed.), The Nematode *Caenorhabditis elegans*. Cold Spring Harbor Laboratory Press, Cold Spring Harbor, NY, pp. 587–606.

Stein, L.D., Bao, Z., Blasiar, D., et al., 2003. The genome sequence of *Caenorhabditis briggsae*: a platform for comparative genomics. PLoS Biol. 1 (2), 166–192.

Teng, Y., Girard, L., Ferreira, H.B., Sternberg, P.W., Emmons, S.W., 2004. Dissection of cis-regulatory elements in the *C. elegans* Hox gen egl-5 promoter. Dev. Biol. 276, 476–492.

Wang, Z.-W., Kunkel, M.T., Wei, A., Butler, A., Salkoff, L., 1999. Genomic organization of nematode 4TM K^+ channels. Ann. N. Y. Acad. Sci. 868, 286–303.

Wenick, A.S., Hobert, O., 2004. Genomic cis-regulatory architecture and trans-acting regulators of a single interneuron-specific gene battery in *C. elegans*. Dev. Cell 6, 757–770.

Woollard, A., Hodgkin, J., 2000. The *Caenorhabditis elegans* fate-determining gene mab-9 encodes a T-box protein required to pattern the posterior hindgut. Genes Dev. 14, 596–603.